Research Article
Geochemistry, Geophysics, Geosystems
DOI 10.1002/2014GC005561

Regional-scale input of dispersed and discrete volcanic ash to the Izu-Bonin and Mariana subduction zones

Rachel P. Scudder and **Richard W. Murray**
Department of Earth & Environment, Boston University, Boston, Massachusetts 02215, USA.

Julie C. Schindlbeck, **Steffen Kutterolf**, and **Folkmar Hauff**
GEOMAR Helmholtz Centre for Ocean Research, Wischhofstrasse 1-3, 24148 Kiel, Germany.

Claire C. McKinley
Department of Earth & Environment, Boston University, Boston, Massachusetts 02215, USA.
Now at: Department of Oceanography, Texas A&M University, College Station, TX 77843, USA.

Corresponding Author: R.P. Scudder, Department of Earth & Environment, Boston University, Boston, Massachusetts 02215, USA (rscudder@bu.edu)

Key Points

- Dispersed ash comprises ~30-35% of the sedimentary input to the IBM subduction system
- The sources and ash layer-to-dispersed ash relationships differ between sites
- Changes in inputs with time indicate strong arc- and climate-related controls

Submitted to G3, August 22, 2014; Re-submitted to G3, October 29, 2014.

This article has been accepted for publication and undergone full peer review but has not been through the copyediting, typesetting, pagination and proofreading process which may lead to differences between this version and the Version of Record. Please cite this article as doi: 10.1002/2014GC005561

Received: Aug 28, 2014; Revised: Oct 31, 2014; Accepted: Nov 03, 2014

Abstract

We have geochemically and statistically characterized bulk marine sediment and ash layers at Ocean Drilling Program Site 1149 (Izu-Bonin Arc) and Deep Sea Drilling Project Site 52 (Mariana Arc), and have quantified that multiple dispersed ash sources collectively comprise ~30-35% of the hemipelagic sediment mass entering the Izu-Bonin-Mariana subduction system. Multivariate statistical analyses indicate that the bulk sediment at Site 1149 is a mixture of Chinese Loess, a second compositionally distinct eolian source, a dispersed mafic ash, and a dispersed felsic ash. We interpret the source of these ashes as respectively being basalt from the Izu-Bonin Front Arc (IBFA) and rhyolite from the Honshu Arc. Sr-, Nd-, and Pb isotopic analyses of the bulk sediment are consistent with the chemical/statistical-based interpretations. Comparison of the mass accumulation rate of the dispersed ash component to discrete ash layer parameters (thickness, sedimentation rate, and number of layers) suggests that eruption frequency, rather than eruption size, drives the dispersed ash record. At Site 52, the geochemistry and statistical modeling indicates that Chinese Loess, IBFA, dispersed BNN (boninite from Izu-Bonin), and a dispersed felsic ash of unknown origin are the sources. At Site 1149 the ash layers and the dispersed ash are compositionally coupled, whereas at Site 52 they are decoupled in that there are no boninite layers, yet boninite is dispersed within the sediment. Changes in the volcanic and eolian inputs through time indicate strong arc- and climate-related controls.

1. Introduction

In regions such as the northwest Pacific Ocean, marine sediment includes abundant volcanic ash and thus information about eruption history, subduction budgets, and regional tectonics. While much work in unraveling volcanic history has focused on discrete ash layers [*e.g.*, Kennett et al., 1977; Carey and Sigurdsson, 1980; Cambray et al., 1995; Kutterolf et al.,

2008], a significant component of ash, that which has been mixed into the sediment as "dispersed ash", has not received as much attention. This dispersed ash is the result of the bioturbation of pre-existing discrete ash layers, the settling of airborne ash through the water, distribution from subaqueous eruptions, and other mechanisms. Unlike ash layers, the dispersed ash component is difficult to differentiate visually from detrital terrigenous clay. Studies based on smear slides and other methods commonly show that it can comprise as much as 30-40 weight percent (wt.%) of the sediment, and such approaches have been enhanced by geochemical and statistical techniques that yield more precise and compositional data [*e.g.*, Straub and Schmincke, 1998; Peters et al., 2000; Scudder et al., 2009]. This dispersed ash is a critical component of the volcanic record and also potentially impacts subduction cycling in terms of the potential for the ash-rich sediment to be returned to the subduction zone itself, along with deeper crustal input [*e.g.*, Plank and Langmuir, 1998; Hauff et al., 2003]. Additionally, the fluid budget and physical properties of subducting sediment will be affected by alteration of the ash material [*e.g.*, Underwood and Pickering, 1996]. Quantifying the amount of dispersed ash will thus assist physical property determinations and subduction zone modeling.

Dispersed ash has been recognized in a number of geologic settings. In the western Caribbean, where the sediment comprises a relatively simple three-component system ($CaCO_3$, terrigenous material, and ash), Peters et al. [2000] observed that the timing of dispersed ash accumulation paralleled that of discrete layers, although the maxima in dispersed ash preceded the Miocene and Eocene maxima in discrete layers by ~2–4 Ma. They hypothesized that the dispersed ash was generated by smaller volcanoes, characteristic of the more juvenile arc, and the larger discrete layers were produced by a mature arc, characterized by larger stratovolcanoes. Carey and Sigurdsson [2000] and Sigurdsson et al. [2000] suggested that these large volcanoes

are capable of injecting large plumes of Central American ash into the upper reaches of the stratosphere, that is, high enough to become entrained in the west-to-east blowing stratospheric wind field (*e.g.*, rather than the familiar east-to-west trade winds of the lower troposphere).

In the northwest Pacific Ocean, Scudder et al. [2009] focused on Ocean Drilling Program (ODP) Site 1149 (see Fig. 1, Fig. S1 for location) in order to test in principle whether a small dataset could be used to identify the differences in source compositions to the bulk sediment even if the bulk sediment was entirely composed of aluminosilicates (in contrast to the more simple Caribbean system). They demonstrated that the accumulation of dispersed ash appears decoupled from the discrete ash layers to a certain extent. Scudder et al. [2009] also documented good correlations between the sources of ash material and the eruptive history of the region, with increases in dispersed ash accumulation corresponding to independently documented increases in volcanism. Those early results from Site 1149 stimulated our current more detailed study of Sites 1149 and 52, to further improve our overall technique (more samples, an enhanced statistical protocol) and to investigate other locations for regional applicability.

Here we present two dispersed ash records from the Izu-Bonin (Site 1149) and Mariana (Site 52) arc system (Fig. 1, Fig. S1). We move beyond the scope of Scudder et al. [2009] by greatly expanding the element menu and sample set, which allows for testing of statistical consistency and also for a more resolved understanding of the geochemical sources. Specifically, the increased sampling resolution in this current study allows us to expand deeper (older) and to increase the number of elements in our analytical suite, which allows for a combination of major and trace elements into a common analytical suite, thus providing more robust conclusions. We also compare and contrast Site 1149 to a new location, DSDP Site 52 east of the northern Mariana Trench, which to our knowledge contains one of the highest amounts of volcanic ash

(non-ignimbrite) in the region. We do not assess the mode of transport of the dispersed ash, rather, our goals are to (a) illustrate the quantitative importance of dispersed ash to the total volcanic record, (b) document our enhanced analytical and statistical approach to the study of dispersed ash, and (c) provide a roadmap to the study of dispersed ash in the marine record of other ocean basins.

We emphasize that studies of dispersed ash will yield less specific outcomes than do those of ash layers, as its extremely fine grain size precludes the type of assessment that can, for example, often relate specific volcanoes to a given ash layer [*e.g.*, Lee et al., 1995; Kutterolf et al., 2008]. For example, most dispersed ash material is very fine silt to clay sized (0-100 μm with significant quantities ~20-30 μm or less) [Huang, 1980; Rose et al 2003]. The major challenge of resolving dispersed ash (from a variety of sources) from eolian inputs (also fine grained, and also perhaps from a variety of sources) in sediment that is entirely composed of aluminosilicate material, is exacerbated by the fact that these collected sources are all from a narrow continuum of compositions. Indeed, historically the composition of upper continental crust has been approximated at various times as ‘granodiorite’, ‘dacite’, or other intermediate composition igneous/volcanic rocks [*e.g.*, Taylor and McLennan, 1985]. While these limitations may be disconcerting when compared to the subtleties that can be resolved by studies of the ash *layers*, we argue here that our studies of the dispersed ash component in the *bulk sediment* represents a significant step forward in understanding the complete record of volcanism that is recorded in pelagic sediment.

2. Dispersed Volcanic Ash in Sediment

2.1 General Chemical Characterization

For samples from ODP Site 1149 seaward of the Izu-Bonin Trench, we have expanded the original relatively small dataset of Scudder et al. [2009] with newly acquired data (see Auxiliary Materials for methods). The upper 180 meters below seafloor (mbsf) at Site 1149 is clay-rich (illite to smectite with decreasing kaolinite downcore [Kawamura and Ogawa, 2002]) with varying amounts of siliceous microfossils and volcanic glass. Volcanic material decreases from Unit I to Unit IIA, and there are no ash layers in Unit IIB where volcanic glass is rare. Ages for Unit I are interpolated based on an age-depth relationship from $^{40}Ar/^{39}Ar$ dating of discrete ash layers [Escutia et al., 2006]. Below Unit I the ages were calculated assuming a linear sedimentation rate of 1.4 m/my based on the age-depth relationship from the bottom of Unit I to the top of Unit IV [Plank et al., 2000].

Downcore concentration profiles and other graphs (Figs. 2, 3; Fig. S2) do not provide clear distinction of the potential sources to the bulk sediment. For example, changes in the concentration of SiO_2 downhole alone appear to indicate that simply mixing between a MORB-like component and Chinese Loess (CL) controls the composition of the sediment. Considering that CL has been extensively documented to be a source to the broad North Pacific region [*e.g.* Hovan et al., 1989; Nakai et al., 1993; Pettke et al., 2000], and that MORB is at least one approximation of a putative mafic end-member, such a first-order interpretation is reasonable. Further inspection, however, of other elements and elemental ratios, such as Ti/Al, indicate that the sediment could be alternatively described as being a mix of CL and an additional, at this point unknown, source with the same chemical composition(s) as that of the discrete ash layers. Indeed, based on Ti/Al alone, there need not be any mafic contribution. Elements such as Nb, however, indicate a more complex mixing history. While other graphical techniques (*e.g.*,

ternary diagrams) provide additional information (Fig. 3), a unique solution to the mixing problem is difficult to generate.

Samples from Site 52 (Mariana Arc) contain extremely high abundances of non-pyroclastic volcanic ash (upwards of 50% volcanic glass in the brown clay). Rotary drilling at Site 52 left only a few ash layers intact (all in the upper 20 mbsf) with no useable age data appropriate for our study [Fischer et al., 1971]. As with Site 1149, elemental abundances and ratios are not sufficient to describe mixing. For example, looking at SiO_2 alone would suggest that the sediment could be explained by mixing of CL and MORB, without any contribution from the volcanic ash. The Ti/Al ratio, however, shows that not to be the case, and suggests that perhaps CL and the ash layers can be mixed to result in the bulk sediment composition. The abundance of Th shows yet a third pattern (Fig. 4).

2.2 Identification of Sources (End-Members) to Bulk Sediment

Multivariate statistical techniques can resolve ambiguities observed in downcore geochemical trends and traditional mixing diagrams [*e.g.*, Pisias et al., 2013]. Q-mode Factor Analysis (QFA) determines the number and broad compositional nature of potential end-member contributions. However, while providing important constraints on the potential end-members, QFA commonly does not yield specifically accurate compositions [Pisias et al., 2013]. To best assess the source compositions we therefore apply Total Inversion (TI), which is a multiple linear regression technique that allows for compositional variation of the end-members.

For both Site 1149 and Site 52, we applied the QFA and Total Inversion (TI) approaches based on the MATLAB scripts from Pisias et al., [2013]. We used a refractory suite of elements predominantly associated with aluminosilicate components (Al, Ti, Sc, Cr, Ni, Nb, La, Th). We emphasize that here we are focused on identifying only the aluminosilicate end-members as

these components make up the bulk of the sedimentary material at these sites and are key to understanding tectonic and climate changes through time. Therefore, the element menu that was selected for these multivariate statistical treatments only targets such aluminosilicate end-members.

In TI the end-member compositions are specified as inputs, allowed to vary slightly to account for compositional variations, and linearly mixed to approximate best the data array. The end-members, being aluminosilicates, fall in the compositional spectrum between, and including, upper crustal (*e.g.*, loess, continental crust, felsic-dacitic ashes, etc.) and more primordial sources (basalts, etc.). As mentioned previously, resolving sources from within this first group is particularly challenging. Using TI, we mixed various combinations of eolian materials (*e.g.*, Chinese Loess [CL], and/or other continental crustal-type compositions) and known compositions of volcanic ash and other sources. Identifying the current composition of likely eolian and continental crustal-type sources is relatively straightforward from the literature, but identification of potential volcanic sources and the composition of older material is more challenging due to the number of potential sources and their potential geochemical evolution through time.

Indeed, a key question in the study of dispersed ash remains “Is the dispersed ash merely discrete layers that have been mixed into the sediment, or does it document an entirely new source(s) of volcanic material?”. Previous workers have largely remained silent on this issue. We here make some first order observations based on the chemistry of the discrete ash layers from the respective sites and whether we can successfully statistically model the bulk sediment composition of each site using its discrete layers as (either all or some) of the volcanic end-

members. If an acceptable model can be generated using (all or some of) the ash layer compositions as end-members, then that is most likely the most appropriate explanation.

Therefore, to determine the composition of potential ash inputs to Sites 52 and 1149 individually, we use compositions from the literature for local/regional arcs (*e.g.*, Izu-Bonin, Honshu, Ryukyu, Kyushu), as well as newly acquired data from the discrete ash layers themselves (Fig. S3). We emphasize that these compositional differences are subtle (*e.g.*, rhyolites from each of these arcs are relatively similar in composition), and because we are dealing with the bulk sedimentary component we cannot exclusively claim a unique solution from the mixing models. Nonetheless, even considering that this work is susceptible to the common limitation facing all provenance studies, namely, that of the assumption that sources themselves are not changing significantly in composition through time, this approach can provide heretofore unrealized constraints on the nature of the volcanic and (terrigenous) eolian contributions to these sediments.

2.2.1 Site 1149, Izu-Bonin

For Site 1149, we performed QFA on the data from Units I and II (n = 89, Table S1). The QFA results indicate that a robust four factors explain 97% of the variability of the bulk sediment (Fig. S4). Using the same refractory element suite as for QFA, the TI independently confirms that four sources yield the smallest statistical residuals, explain more than 99% of the dataset's variability, and on an element-by-element basis have the strongest r-values throughout the model (Table S5). In particular, there is no combination of three sources that yield better statistical results than those based on four end-members, which reinforces the importance of working with a large sample set. The four sources that best explain the bulk sediment are CL, rhyolitic ash from the Honshu arc, mafic ash from the Izu-Bonin Front Arc (IBFA), and a second eolian dust

(termed "Eolian 2"). We arrived at this specific group of sources by mixing many possible combinations of likely inputs (Table S2), and by making reasonable assumptions based on geological constraints as to where the sources could potentially have originated. While these compositions are based on the current composition of the source, that TI allows for variability of the sources should account for small changes in the compositional evolution of the source material that may have occurred over time.

The radiogenic isotopes of Sr, Nd, and Pb at Site 1149 provide another mechanism by which the aluminosilicate contributions to the bulk sediment can be evaluated. We tested our TI mixing results for Site 1149 by mixing the amount of each end-member along with its inferred (for sources such as CL, from the literature) or measured (for mafic and felsic ash layers from Site 1149) isotopic composition to generate a predicted bulk sediment isotopic ratio (Fig. S5). For each isotope system we then compared this synthetically generated mixed isotope ratio to the measured bulk sediment isotopic ratio. While limited by a small sample size, the nature of bulk sedimentary isotopic analysis, and diagenesis, the Sr-, Nd-, and Pb isotopic results are consistent with the bulk sediment resulting from mixing of these sources.

Considering these four end-members for Site 1149, we found that including in the TI model the average composition of IBFA ash, instead of that of the mafic ash layers, consistently explained a higher percent of the variability and resulted in lower (better) residuals. Elemental r-values for the two models show that the model with the mafic layers has higher r-values for Ni and La, while exchanging IBFA for the mafic layers yields slightly higher r-values for Ti, Sc, Cr, and Th. Because these modeled results are close in quality, and cognizant of the challenges with working in fine-grained bulk sediment, we interpret that the mafic ash layers at Site 1149 are from IBFA. Similarly, if we include rhyolitic ash from the Honshu Arc (hereafter, Honshu

Rhyolite, "HR") instead of the felsic ash layers, the residuals are consistently lower (a better fit). Other rhyolites from other arcs do not model as well as does HR. The r-values for Sc are lower (worse) when including HR, although the r-values for the other 7 elements in the menu are the same or higher. Collectively, these differences are slight. Thus, we suggest that HR is the most likely source of the felsic ash layers.

The interpretation of a distal end-member of dispersed ash is consistent with previous studies that have found Ryukyu and/or Honshu volcanic material in Izu-Bonin sediments. Egeberg et al. [1992] interpreted trace element, Sr-, and Nd isotopic signatures in certain ash layers at ODP Site 792 (located on the eastern margin of the Izu-Bonin forearc basin between the active volcanic arc and the Izu-Bonin Trench, Fig. 1) as variously deriving from the Ryukyu and Honshu arcs. Scudder et al. [2009] interpreted one of the dispersed ash components at Site 1149 as being broadly consistent with Ryukyu dacite. For the purposes of our current study and given the tolerances of working with dispersed ash, however, there is no substantive difference as to whether this dispersed felsic component derives from the Honshu or the Ryukyu arc or if it is dacitic or rhyolitic. Our key finding is that it is a broadly felsic distal component that does not come from the proximal Izu-Bonin region. After considering the expanded element menu and larger sample set, we suggest that Honshu Arc is the most likely source.

The fourth end-member, named "Eolian 2", results from including "Upper Continental Crust" [UCC; Taylor and McLennan, 1985] in the models. This UCC generally results in better statistical fitting through a variety of scenarios, despite its low abundance. For example, using a dacitic composition (either a generic "dacite" or specific dacites from Ryukyu, Honshu, and/or Izu-Bonin) for this fourth end-member yielded poorer results. We further tried many different combinations of rhyolitic and dacitic end-members along with CL and IBFA, and the best

statistical result includes HR (as above) and UCC. This is a consistent result through many sensitivity tests, even given that UCC is not that compositionally distinct from "dacite". Because this upper continental crustal material can only reach Site 1149 by eolian transport, we interpretatively name it "Eolian 2", and its importance will be explored more fully elsewhere.

2.2.2 Site 52, Northern Mariana Arc

Applying the same principles and chemical suite to the sediment record at Site 52 (Fig. S6) indicates that four sources explain 99% of the data variability. However, two of the factors at Site 52 closely resemble two found at Site 1149, while the other two do not (Figs. S4, S6). This is expected given the separation of these two sites by ~500 km and ~5° of latitude. Despite the mixing imposed by rotary drilling and other factors that may have destroyed individual ash layers, the dispersed ash record from Site 52 preserves important geological information and reinforces the importance of the statistical methods. Indeed, Jutzeler et al. [2014] note that drilling related core disturbance can create "substantial artificial stratigraphic gaps" which can be overcome through the use of these methods.

Additionally, at Site 52 we observe that, in contrast to Site 1149 where the ash layer compositions can be mixed to explain the dispersed ash component, the chemical composition of the layers alone when mixed with CL and other potential eolian "crustal" sources does not explain the aluminosilicate chemistry of the bulk sediment. Rather, Site 52's mafic ash (termed "Mafic52"), Site 52's felsic ash ("Felsic52"), and an additional component, average Izu-Bonin boninite (BNN), are required. Including BNN is required by both the bulk sediment composition as well as the statistical models (Fig. S7). Exchanging IBFA for the mafic ash (Mafic52) yields similar results, and we thus interpret the mafic layers as being IBFA. Notably, mixing any of the dacitic or rhyolitic ashes from nearby arcs does not adequately explain the data. Therefore, the

best component mix to model sediment composition at Site 52 is CL, Mafic52, Felsic52, and BNN.

We acknowledge that calling for a boninite to be contributing material to Site 52, back particularly when it was located to the east distal from the current arc (Fig. S1), is unusual. However, the high bulk concentrations of Ni and Cr and low concentrations of Al, as well as the modeling results, requires such a source. To our knowledge, there is no other composition of an aluminosilicate component that can fulfill these constraints. In parallel to some of the points made previously, we are not necessarily saying that the boninite material now found in Site 52 sediment originated specifically from Izu-Bonin, but instead that a boninite from some source is included. We use boninite from Izu-Bonin as the end-member composition because it as good a boninite as any, compositionally-speaking, to use in our models of the fine-grained bulk sediment. This is explored further below.

3. Dispersed Ash, Discrete Ash Layers, Loess, and Other Eolian Inputs

Successfully constraining the CL, HR, IBFA, and Eolian 2 inputs to Site 1149 allows us to assess volcanic- and climate-related processes. The dispersed ash mass accumulation rate (MAR) most closely tracks the simple number of discrete ash layers per 1 my, and also follows the ash layer sedimentation rate (Fig. 5). Both of those discrete ash parameters are likely controlled by the frequency of explosive eruptions. The dispersed MAR does not follow the *thickness* of the ash layers, and therefore we interpret that the dispersed ash record is not related to eruption size. Although a thick ash layer may result from either a large eruption or a nearby eruption (or both), because Site 1149 is tectonically approaching the Izu-Bonin Arc through time (Fig. S1) we would predict that thicker ash layers would be more prevalent in the younger (shallower) sections of the stratigraphy deposited when the site was progressively nearer the arc.

However, this is not strongly observed in the younger discrete layer record, which is where the dispersed MAR shows its largest increase. Therefore, we conclude the dispersed ash is indeed responding to overall volcanic activity, which will be recorded by the combined records of dispersed ash and the ash layers, and not just eruption size, which would have been recorded by ash layer thickness.

Additionally, if the dispersed ash record was dominantly caused by bioturbation of now destroyed ash layers, we would expect that where the number of ash layers is low there would be more abundant dispersed ash. This is not observed. We therefore interpret that the dispersed record reflects periods of enhanced regional/global volcanism, subaqueous volcanism, and/or other mixing of subaerial volcanic material (*e.g.*, eroded from the arc).

We now consider the tectonic- and arc evolution of the region. At Site 1149, there is no dispersed ash accumulation from ~55-50 Ma (Figs. 5,6). This is followed by a 10 My interval centered on ~45 Ma through which dispersed ash increased from ~50-45 Ma, and then decreased from 45 Ma to nearly zero at ~40 Ma. This period broadly corresponds to IBM arc initiation at ~52-50 Ma [*e.g.*, Reagan et al., 2013] and the ~50-47 Ma bend in the Hawaiian-Emperor chain [O'Connor et al., 2013, and references therein] that may reflect large scale tectonic reorganizations caused by India-Asia collision (53-51 Ma) [Najman et al., 2010]. From this time to ~6 Ma, dispersed ash showed a gradual yet consistent increase. From ~6 Ma and younger, and along with the most rapid increase at ~3 Ma, dispersed accumulation increased by essentially an order of magnitude.

If we separate the two types of dispersed ash we can interpret these changes in accumulation rate in terms of arc history. Within the tolerances of the age model and scaled to the questions that we are asking, we observe that HR is the dominant dispersed ash. This

indicates that, despite it being relatively far away, the Honshu Arc still contributed significant ash to locations east of Izu-Bonin. Such putative eruptions could have been large, yet Site 1149's distal location at the time resulted in only thin layers that were subsequently mixed into the bulk sediment. Alternatively, the dispersed ash could merely represent an increase in general deposition of ash from the atmosphere. Regardless, the 10 Myr increase in total dispersed ash accumulation in the interval centered on ~45 Ma appears to be driven by this HR source. Although the timing and history of this arc system is complex, the MAR of HR through the younger portions of the record is consistent with the tectonic history of the Honshu Arc. As a result of spreading of the Japan Sea, in the north, southwestern Japan began to rotate at ~15 Ma as the Izu-Bonin Arc moved offshore to the Kii Peninsula. Simultaneously, the Shikoku Basin spreading ridge activated. From ~12-8 Ma, the Izu Arc ceased motion as it entered its current position and from ~11-6 Ma volcanic activity in southwestern Japan ceased almost entirely. Following this period of decreased activity, volcanism increased again at ~6 Ma (Kimura et al., 2014).

The model further documents a gradual increase in IBFA volcanism from ~18-10 Ma, and a burst of activity from ~4.5-3 Ma followed by a steady increase beginning at ~2 Ma (Fig. 6). These temporal changes are well documented in the tectonic record of Izu-Bonin [*e.g.*, Cambray et al., 1995]. That the dispersed record faithfully records this volcanic history highlights the necessity of considering dispersed ash in any complete assessment of volcanic activity.

Chinese Loess drives the dust record in the sediment, consistent with long-standing understandings of this important source to the region [*e.g.*, Rea, 1994]. Differentiating this material from volcanic ash using our technique speaks to the robustness of the overall strategy

and its applicability to a variety of locations. Moreover, the presence of an important second non-ash, terrigenous source ("Eolian 2") is intriguing. The long-term decrease in Eolian 2 from ~55 Ma to ~20 Ma may have important implications for the climatic evolution of the Asian interior, although it does not appear to be responding to any one specific event. The observed change at ~25-20 Ma, a tectonically and climactically active time in Earth's past, indicates that the two dust sources are best interpreted in the context of their dual occurrence. These results will be presented in greater detail elsewhere.

The lack of age control at Site 52 precludes calculating accumulation rates, therefore, we are unable to address definitively questions such as whether the changes in sources are related to plate tectonic reorganization. Similarly, we cannot address whether the increase in BNN *abundance* would parallel in increase in BNN *accumulation* from 30 mbsf and younger as Site 52 approached the Mariana fore-arc.

Site 52 nonetheless presents some key similarities and differences from Site 1149. First, the total amount of dispersed ash (regardless of composition) at both sites is very high, averaging 30 +/- 17 wt. % at Site 1149 and 36 +/- 18 wt. % at Site 52. Second, whereas at Site 1149 there are two ashes (HR, IBFA) found both as layers and as dispersed, at Site 52 there are at least three ashes since the layers appear to be IBFA and Felsic52, and the dispersed ash is IBFA, Felsic52, and BNN. Thus, at Site 52, the ash layers and the dispersed ash are partially decoupled. Given that boninite has commonly been recognized in fore-arc settings this may explain the very low abundance observed at Site 52 (Fig. 7). We also note that dispersed ash can be generated by subaqueous eruptions [Fiske et al 2001; Fujibayashi and Sakai, 2003]. The source of Felsic52 remains unclear, although given that the compositions of end-members must be known for TI analysis it seems reasonable to interpret that Felsic52 is from a volcanic source with an

intermediate composition that has yet to be presented in the literature. Third, at Site 52 the Eolian 2 source found at Site 1149 is not required by the data or models, which may reflect the differences in latitude between the two sites and associated subtle differences in eolian sources from mainland Asia.

4. Summary

Dispersed volcanic ash is a significant component of the IBM sediment system, accounting for ~30-35 wt.% of the bulk sediment input to the trench. There are two distinct compositions of eolian sources to Site 1149 (Chinese Loess, Eolian 2). This second input most likely represents eolian sources in Asia, and our approach provides compelling evidence that it is distinct from "classic" Chinese Loess.

Multivariate statistical treatments at Site 1149 identifies that the current compositions of CL, Eolian 2, IBFA mafic ash, and Honshu Rhyolite best explain the bulk sedimentary composition. Sr-, Nd-, and Pb isotopic analyses are consistent with this interpretation. At Site 52, four end-members also comprise the bulk sediment, and are Chinese Loess, IBFA, Felsic52, and a boninite (BNN). Notably, boninite ash layers were not recovered by rotary drilling at Site 52, yet the bulk composition requires boninite to be present in the mix. Therefore, at Site 52 the ash layers and the dispersed ash components appear partly decoupled. Also, at Site 52 there appears to be no second eolian source.

At Site 1149 (and drilling recovery at Site 52 was too poor to allow this analysis), comparison of the dispersed MAR to a series of ash layer parameters indicates that the number of ash layers closely tracks the dispersed ash MAR, and thus the *frequency*, rather than the *size*, of eruptions is driving the dispersed ash record. The MAR patterns are consistent with published

eruption records of both the Izu-Bonin and Honshu arcs, and they correlate reasonably well with the known tectonic evolution of both arc systems. Finally, this geochemical and statistical approach allows us to discriminate between individual sources within an array of aluminosilicate contributions (multiple ash types, and several different eolian inputs) at these two sites, suggesting that this approach is promising for other oceanic regions.

Acknowledgements

All data for this paper is available in the Auxiliary Material.

RPS, RWM, and CCM thank the US IODP and NSF OCE-0958002 for financial support, and T. Ireland, A.G. Dunlea, R. Lauzon, and J.W. Sparks. JS and SK thank the German Research Foundation (Ku-2685/2-1; 1-2), IODP Germany for funding the position of JS and the microanalytical work, and M. Thöner and K. Junge for laboratory assistance. We thank D. Cardace and M. Underwood for their detailed and insightful comments.

References Cited

Cambray, H., Pubellier, M., Jolivet, L., and Pouclet, A., 1995, Volcanic activity recorded in deep-sea sediments and the geodynamic evolution of western Pacific island arcs, in Taylor, B., and Natland, J., eds., Active Margins and Marginal Basins of the Western Pacific: Washington, DC, American Geophysical Union Geophysical Monograph 88, p. 97–124.

Carey, S.N., and Sigurdsson, H., 1980. The Roseau ash: Deep-sea tephra deposits from a major eruption on Dominica, Lesser Antilles arc. Journal of Volcanology and Geothermal Research, 7: 67-86.

Carey, S.N. and Sigurdsson, H., 2000, Grain size of Miocene volcanic ash layers from sites 998, 999, and 1000; implications for source areas and dispersal. Proceedings of the Ocean Drilling Program, Scientific Results, Volume 165 College Station, TX, p. 101-113.

Egeberg, P.K., Brunfelt, A.O., and Stabel, A.S., 1992, Characterization and correlation of megascopic tephras in Site 792 cores from the Izu-Ogasawara forearc basin (Japan) by trace elements and 87Sr/86Sr and 143Nd/144Nd isotopes, in Taylor, B., Fujioka, K., et al., Proceedings of the Ocean Drilling Program, Scientific Results, Volume 126: College Station, TX, p. 457–465.

Escutia, C., Canon, M., and Gutierrez-Pastor, J., 2006. Data report: $^{40}Ar/^{39}Ar$ chronology of discrete ash layers in the northwestern Pacific: ODP Sites 1149 and 1179, *in* Ludden, J.N., Plank, T., and Escutia, C. (Eds.), Proceedings of the Ocean Drilling Program, Scientific Results, Volume 185: College Station, TX (Ocean Drilling Program), 1–20. doi:10.2973/odp.proc.sr.185.015.2006

Fischer, A. G., et al., 1971, Initial Reports of the Deep Sea Drilling Project, Volume VI: Washington, D.C., U.S. Government Printing Office, p. 247-290.

Fiske, R.S., Naka, J., Iizasa, K., Yuasa, M., and Klaus, A., 2001. Submarine silicic caldera at the front of the Izu-Bonin arc, Japan: voluminous seafloor eruptions of rhyolite pumice. Geological Society of America Bulletin 113: 813-824.

Fujibayashi, N. and Sakai U. 2003. Vesiculation and eruption processes of submarine effusive and explosive rocks from the Middle Miocene Ogi basalt, Sado Island, Japan: Explosive Subaqueous Volcanism, Amer. Geophys. Union Monograph, v. 140, p. 259–272.

Hauff, F., Hoernle, K., Schmidt, A., 2003, Sr-Nd-Pb composition of Mesozoic Pacific oceanic crust (Site 1149 and 801, ODP Leg 185): Implications for alteration of ocean crust and

the input into the Izu-Bonin-Mariana subduction system: Geochemistry Geophysics Geosystems, v.4, 8913.

Huang, T.C., 1980. A volcanic sedimentation model: implications of processes and responses of deep-sea ashes. Marine Geology, 38: 103-122.

Hovan, S.A., Rea, D.K., Pisias, N.G., and Shackleton, N.J., 1989, A direct link between the China loess and marine ^{18}O records: aeolian flux in the north Pacific: Nature, v. 340, p. 296–298

Jutzeler, M., White, J.D.L., Talling, P.J., McCanta, M., Morgan, S., Le Friant, A., and Ishizuka, O., 2014, Coring disturbances in IODP piston cores with implications for offshore record of volcanic events and the Missoula megafloods: Geochemistry Geophysics Geosystems, accepted article.

Kawamura, K., and Ogawa, Y., 2002, Progressive microfabric changes in unconsolidated pelagic and hemipelagic sediments down to 180 mbsf, northwest Pacific, ODP Leg 185, Site 1149, *in* Ludden, J.N., Plank, T., and Escutia, C. (Eds.), Proceedings of the Ocean Drilling Program, Scientific Results, Volume 185: College Station, TX: College Station, TX (Ocean Drilling Program), p. 1–29. doi:10.2973/odp.proc.sr.185.003.2002

Kennett, J.P., McBirney, A.R. and Thunell, R.C., 1977, Episodes of cenozoic volcanism in the circum-pacific region: Journal of Volcanology and Geothermal Research, v. 2 n. 2, p. 145.

Kimura, G., Hashimoto, Y., Kitamura, Y., Yamaguchi, A., and Koge, H., 2014, Middle Miocene swift migration of the TTT triple junction and rapid crustal growth in southwest Japan: A review: Tectonics, v. 33, n. 7, p. 1219–1238.

Kutterolf, S., Freundt, A., and Perez, W., 2008, Pacific offshore record of plinian arc volcanism

in Central America: 2. Tephra volumes and erupted masses: Geochemistry Geophysics Geosystems, v. 9, no. 2.

Lee, J., R. J. Stern, and S. H. Bloomer, 1995. Forty million years of magmatic evolution in the Mariana arc: The tephra glass record, Journal of Geophysical Research, 100(B9), 17,671–17,687.

Najman, Y., Appel, E., Boudagher-Fadel, M., Bown, P., Carter, A., Garzanti, E., Godin, L., Han, J., Liebke, U., Oliver, G., Parrish, R., and Vezzoli, G., 2010, The timing of India-Asia collision: sedimentological, biostratigraphic and palaeomagnetic constraints: Journal of Geophysical Research v. 115, n. B12416.

Nakai, S., Halliday, A.N., and Rea, D.K., 1993. Provenance of dust in the Pacific Ocean: Earth and Planetary Science Letteers, v. 119, p. 143–157.

O'Connor, J.M., Steinberger, B., Regelous, M., Koppers, A.P., Wijbrans, J.R., Haase, K.M., Stoffers, P., Jokat, W., and Garbe-Schönberg, D., 2013, Constraints on past plate and mantle motion from new ages for the Hawaiian-Emperor Seamount Chain: Geochemistry Geophysics Geosystems, v. 14, n. 10, p. 4564- 4584.

Peters, J.L., Murray, R.W., Sparks, J.W., and Coleman, D.S., 2000. Terrigenous matter and dispersed ash in sediment from the Caribbean Sea: results from Leg 165, *in* Leckie, R.M., Sigurdsson, H., Acton, G.D., and Draper, G., Proceedings of the Ocean Drilling Program, Scientific Results, Volume 165: College Station, TX, p. 115–124.

Pettke, T., Halliday, A.N., Hall, C.M., and Rea, D.K., 2000, Dust production and deposition in Asia and the north Pacific Ocean over the past 12 Myr: Earth and Planetary Science Letters, v. 178, p. 397-413.

Pisias, N.G, Murray, R.W, and Scudder, R.P, 2013, Multivariate statistical analysis

and partitioning of sedimentary geochemical data sets: General principles and specific MATLAB scripts: Geochemistry Geophysics Geosystems, v. 14, no. 10, p. 4015-4020.

Plank, T. and Langmuir, C.H., 1998, The chemical composition of subducting sediment and its consequences for the crust and mantle: Chemical Geology, v. 145, n. 3-4, p. 325-394.

Plank, T., Ludden, J.N., Escutia C., et al., 2000, Proceedings of the Ocean Drilling Program, Initial Report, Volume 185: College Station, TX (Ocean Drilling Program). doi:10.2973/odp.proc.ir.185.2000

Rea, D., 1994, The paleoclimatic record provided by eolian deposition in the deep-sea - the geologic history of wind: Reviews of Geophysics, v. 32, no. 2, p. 159-195.

Reagan, M.K., McClelland, W.C., Girard, G., Goff, K.R., Peate, D.W., Ohara, Y., and Stern, R.J., 2013, The geology of the southern Mariana fore-arc crust: implications for the scale of Eocene volcanism in the western Pacific: Earth Planetary Science Letters, v. 380, p. 41–51.

Rose, W.I., Riley, C.M. and Dartevelle, S., 2003, Sizes and shapes of 10-Ma distal fall pyroclasts in the Ogallala Group, Nebraska. Journal Of Geology, 111(1): 115-124.

Scudder, R.P, Murray, R.W, and Plank, T., 2009, Dispersed ash in deeply buried sediment from the northwest Pacific Ocean: An example from the Izu-Bonin arc (ODP Site 1149): Earth and Planetary Science Letters, v. 284, no. 3-4, p. 639-648.

Sigurdsson, H. et al., 2000, History of circum-Caribbean explosive volcanism; 40Ar/39Ar dating of tephra layers. Proceedings of the Ocean Drilling Program, Scientific Results, Volume 165: College Station, TX, p. 299-314.

Straub, S.M. and Schmincke, H.U., 1998, Evaluating the tephra input into Pacific Ocean

sediments: distribution in space and time: Geologische Rundschau, v. 87, no. 3, p. 461-476.

Taylor, S.R. and McLennan, S.M., 1985, The continental crust: Its composition and evolution. Blackwell Scientific Pub., 328 pp.

Underwood, M.B. and Pickering, K.T., 1996, Clay mineral provenance, sediment dispersal patterns, and mudrock diagenesis in the Nankai accretionary prism, southwest Japan: Clays and Clay Minerals, v. 44, p. 339-356.

Figure Captions

Fig. 1. Locations and lithologies of ODP Site 1149 and DSDP Site 52. Arrow represents generalized path of source materials (eolian and ash). Backtrack paths and location information are in Fig. S1. ODP Site 792 also shown (see text).

Fig. 2. Site 1149, representative compositions (Table S1) and elemental ratios plotted with depth. Sources for end-member data can be found in Table S2. Different elemental abundances and ratios suggest contrasting mixtures of representative potential end-member compositions, indicating need for multivariate treatment of large element menu.

Fig. 3. Ternary diagrams showing potential end-members and bulk sediment chemistry at Site 1149. Contrasting patterns indicate a variety of mixing relationships could yield the bulk chemistry. **Left.** Some of the samples in Unit IIB fall outside the bounds of end-members, particularly towards the Th apex. **Right.** All samples fall in field circumscribed by all potential end-members.

Fig. 4. Downcore profiles from Site 52 (data in Table S1).

Fig 5. Site 1149. The accumulation rate of total dispersed ash (that is, the accumulation sum of IBFA and HR, gray shaded with filled circles in $g/cm^2/kyr$, and is the same in each panel) plotted against parameters associated with the sedimentation of discrete ash layers per 1 Ma (open circles, and are different in each panel as shown in the bottom x-axis labels). Lithologic units plotted on the right in each panel. A moving 1 Ma window was chosen to bin each discrete ash layer parameter to approximate the resolution of the modeled dispersed ash record.

Fig. 6. Individual data and three-point averages of MARs of each end-member. Eolian sources on left, dispersed ash on right. Insets focus on the younger portion of each record. Note color-coded different x-axis scales and labels. A few dots are covered in left panel by the inset. Data in Table S7.

Fig. 7. Modeled abundances (wt. %) of end-members contributing to the bulk sediment, Site 52 (Table S7). Note similarity of the modeled BNN boninite here (expanded view on right) with the Ni/Al ratio of Figure DR9.

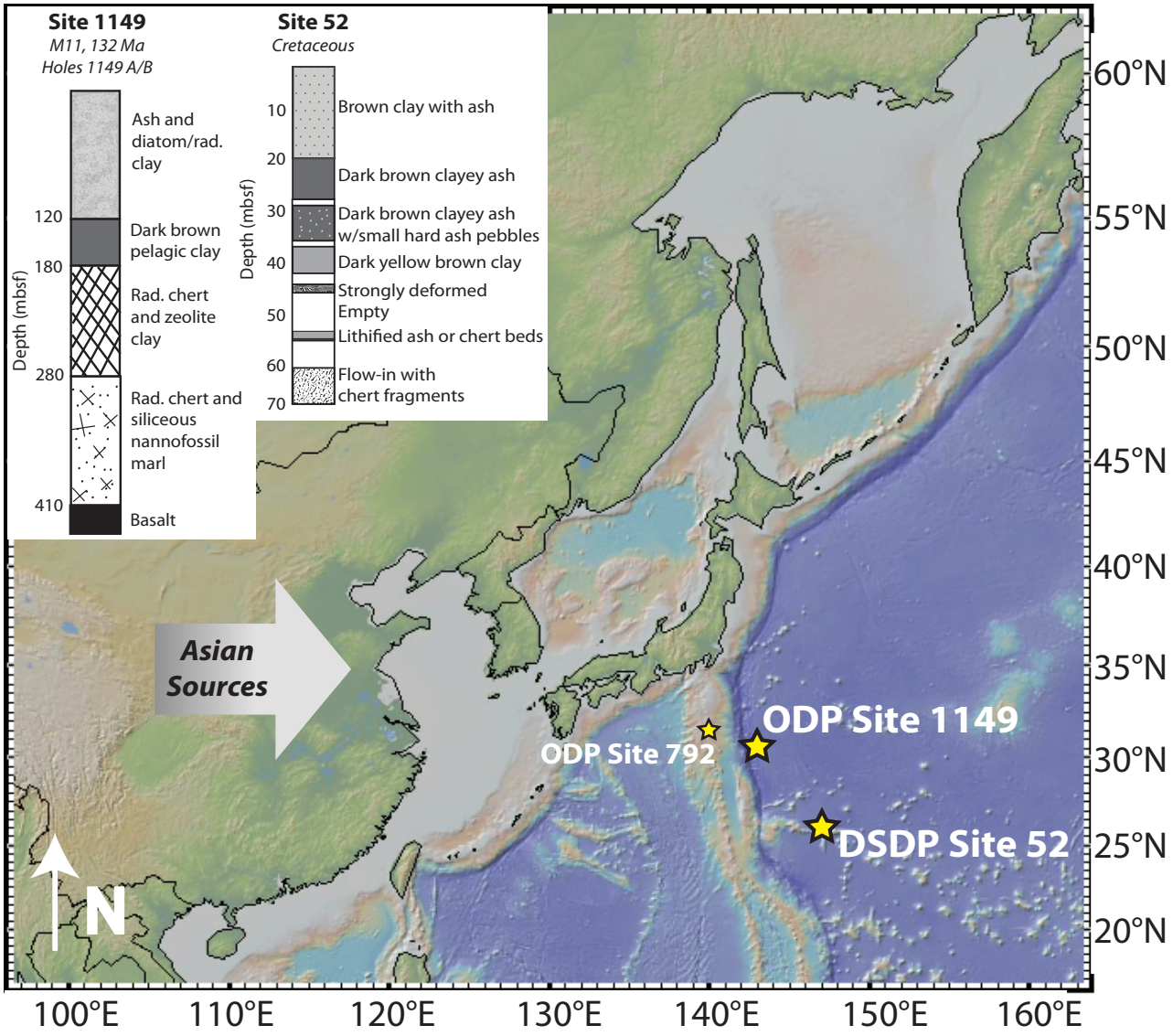
Site 1149
M11, 132 Ma
Holes 1149 A/B
Depth (mbsf)
120
180
280
410
Ash and diatom/rad. clay
Dark brown pelagic clay
Rad. chert and zeolite clay
Rad. chert and siliceous nannofossil marl
Basalt
Site 52
Cretaceous
Depth (mbsf)
10
20
30
40
50
60
70
Brown clay with ash
Dark brown clayey ash
Dark brown clayey ash w/small hard ash pebbles
Dark yellow brown clay
Strongly deformed
Empty
Lithified ash or chert beds
Flow-in with chert fragments
Asian Sources
ODP Site 1149
ODP Site 792
DSDP Site 52
N
60°N
55°N
50°N
45°N
40°N
35°N
30°N
25°N
20°N
100°E
110°E
120°E
130°E
140°E
150°E
160°E

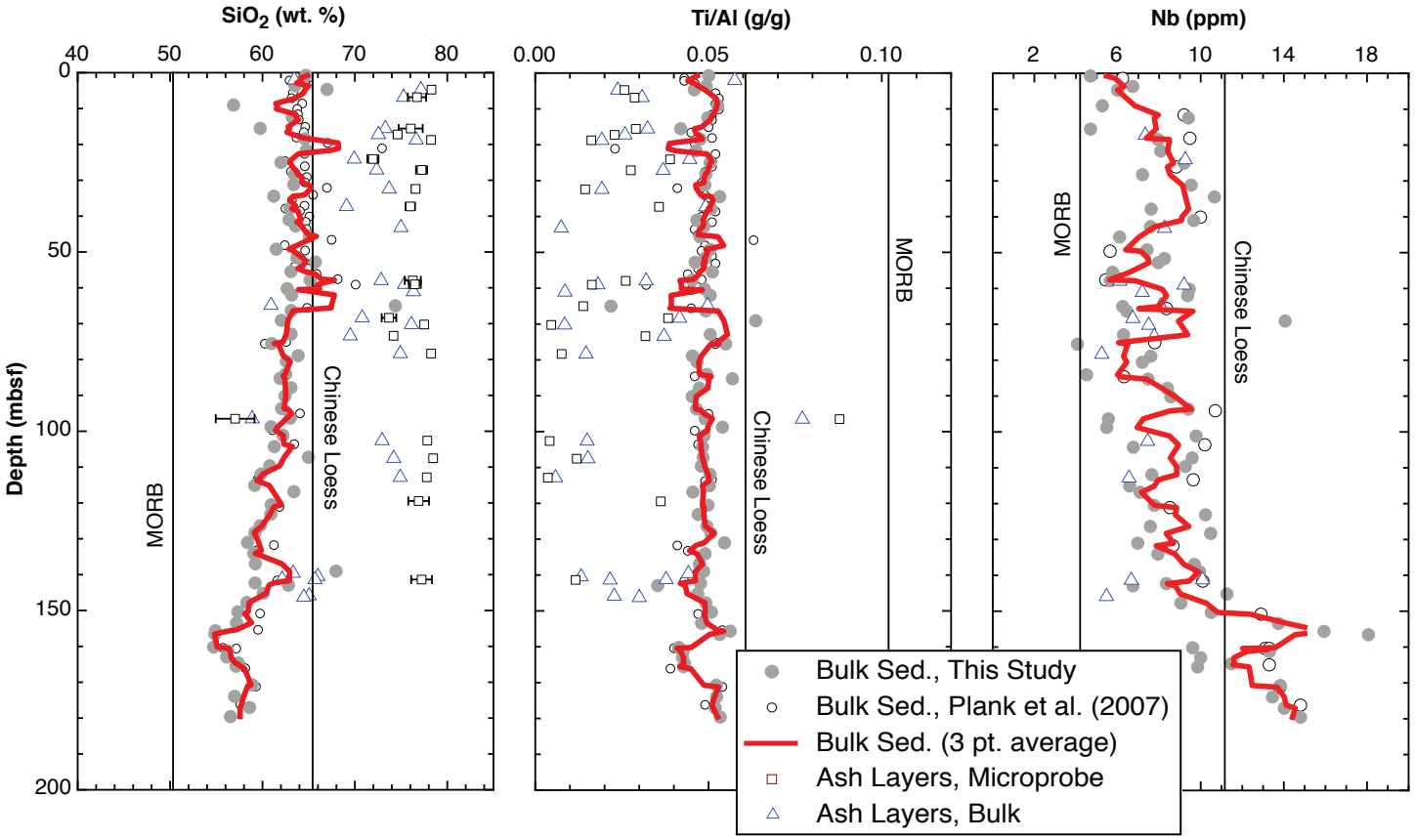
SiO2 (wt. %)
Ti/Al (g/g)
Nb (ppm)
Depth (mbsf)
MORB
Chinese Loess
Bulk Sed., This Study
Bulk Sed., Plank et al. (2007)
Bulk Sed. (3 pt. average)
Ash Layers, Microprobe
Ash Layers, Bulk

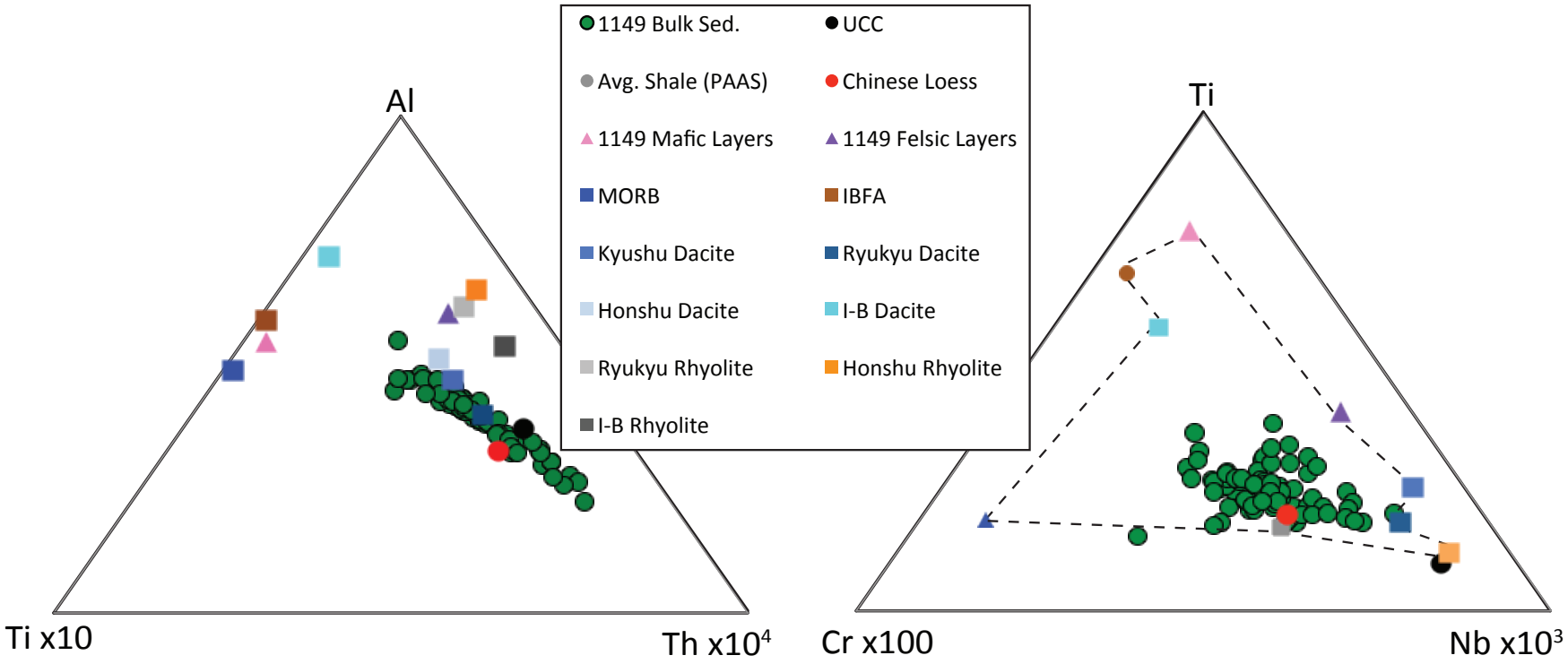
1149 Bulk Sed.
UCC
Avg. Shale (PAAS)
Chinese Loess
1149 Mafic Layers
1149 Felsic Layers
MORB
IBFA
Kyushu Dacite
Ryukyu Dacite
Honshu Dacite
I-B Dacite
Ryukyu Rhyolite
Honshu Rhyolite
I-B Rhyolite
Al
Ti x10
Th x10^4
Ti
Cr x100
Nb x10^3

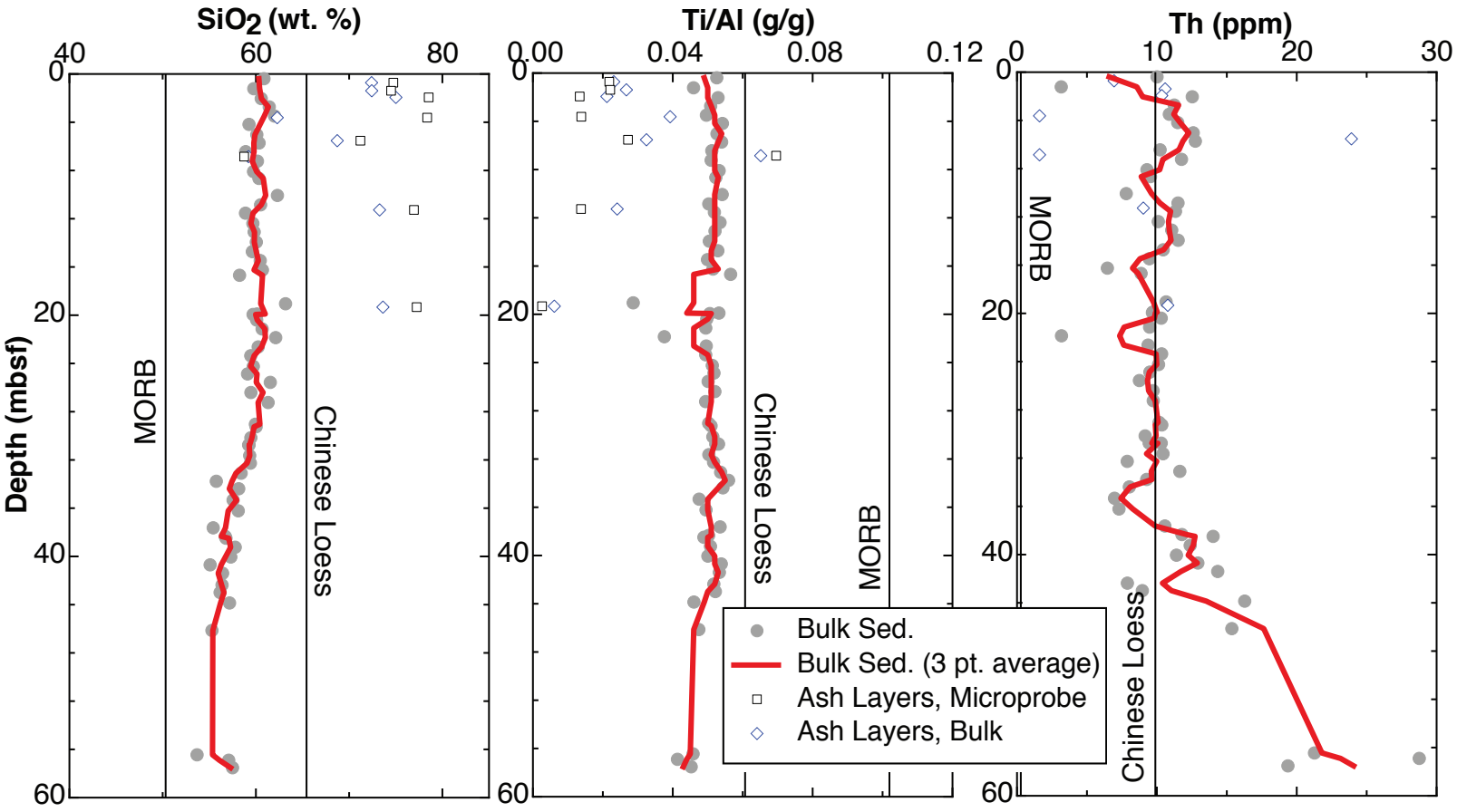
SiO2 (wt. %)
40
60
80
Ti/Al (g/g)
0.00
0.04
0.08
0.12
Th (ppm)
0
10
20
30
Depth (mbsf)
0
20
40
60
MORB
Chinese Loess
Chinese Loess
MORB
MORB
Chinese Loess
Bulk Sed.
Bulk Sed. (3 pt. average)
Ash Layers, Microprobe
Ash Layers, Bulk

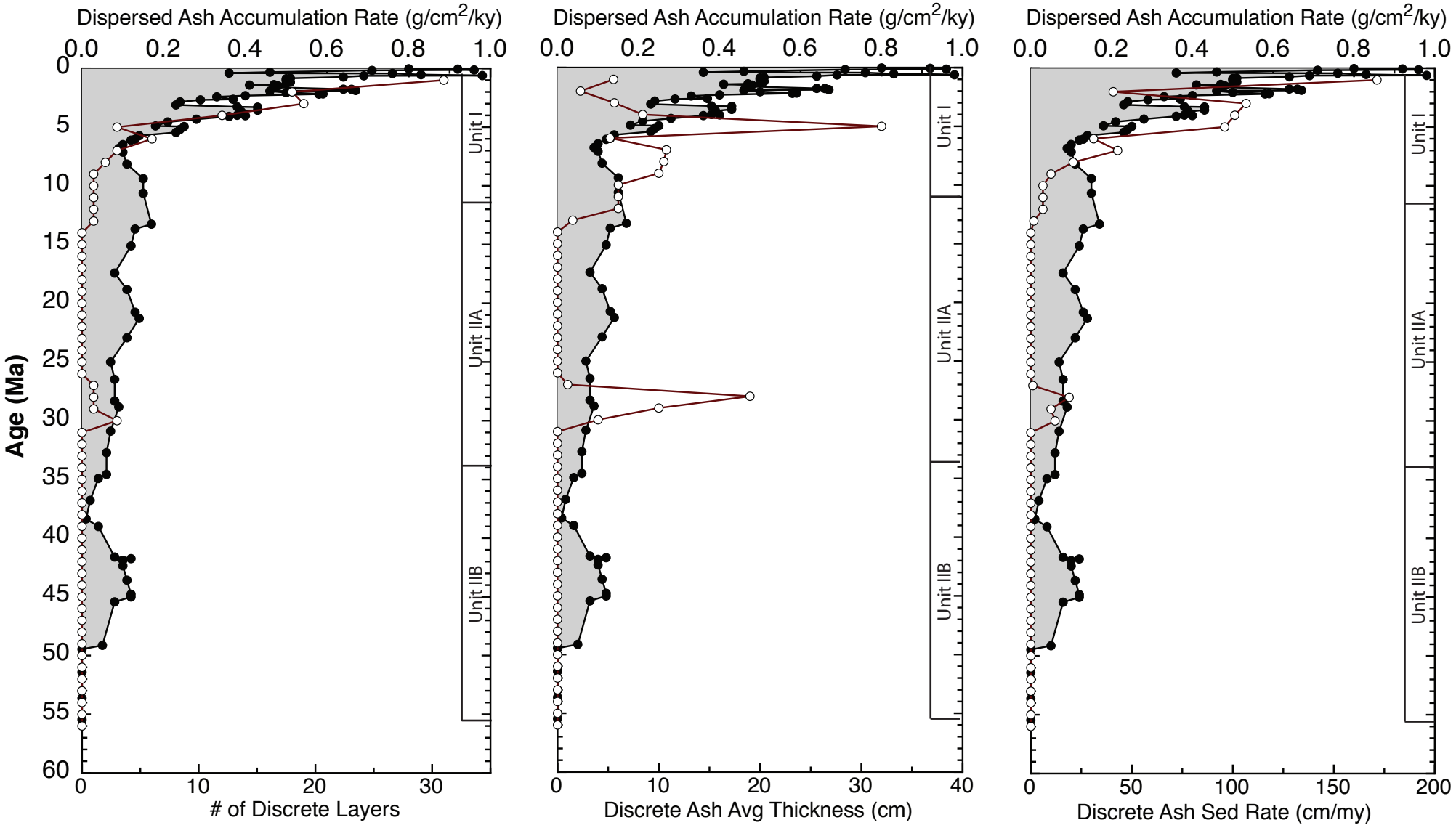
Dispersed Ash Accumulation Rate (g/cm2/ky)
0.0
0.2
0.4
0.6
0.8
1.0
Age (Ma)
0
5
10
15
20
25
30
35
40
45
50
55
60
Unit I
Unit IIA
Unit IIB
0
10
20
30
# of Discrete Layers
Dispersed Ash Accumulation Rate (g/cm2/ky)
Unit I
Unit IIA
Unit IIB
0
10
20
30
40
Discrete Ash Avg Thickness (cm)
Dispersed Ash Accumulation Rate (g/cm2/ky)
Unit I
Unit IIA
Unit IIB
0
50
100
150
200
Discrete Ash Sed Rate (cm/my)

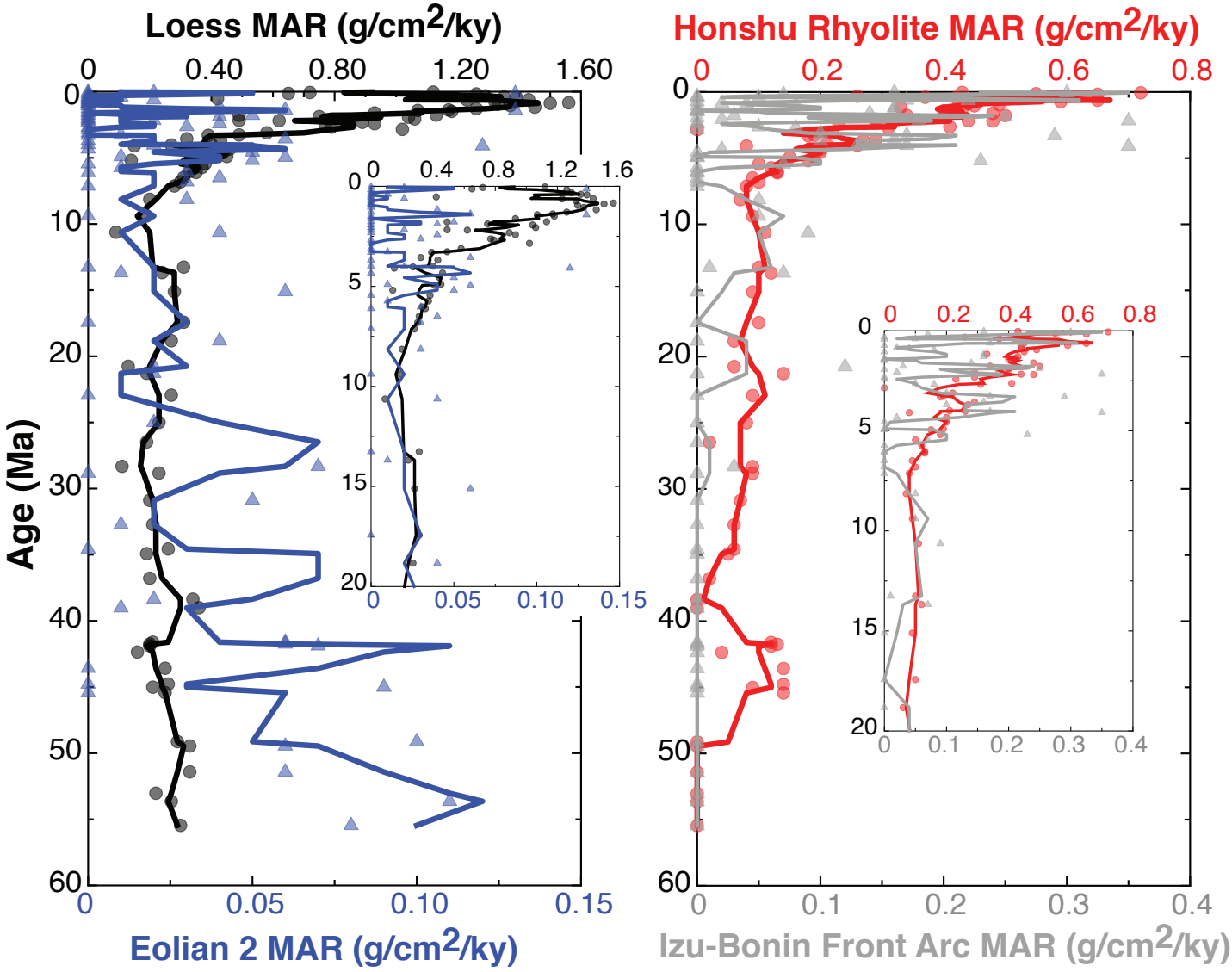
Loess MAR (g/cm2/ky)
0
0.40
0.80
1.20
1.60
Age (Ma)
0
10
20
30
40
50
60
0
0.05
0.10
0.15
Eolian 2 MAR (g/cm2/ky)
Honshu Rhyolite MAR (g/cm2/ky)
0
0.2
0.4
0.6
0.8
0
0.1
0.2
0.3
0.4
Izu-Bonin Front Arc MAR (g/cm2/ky)

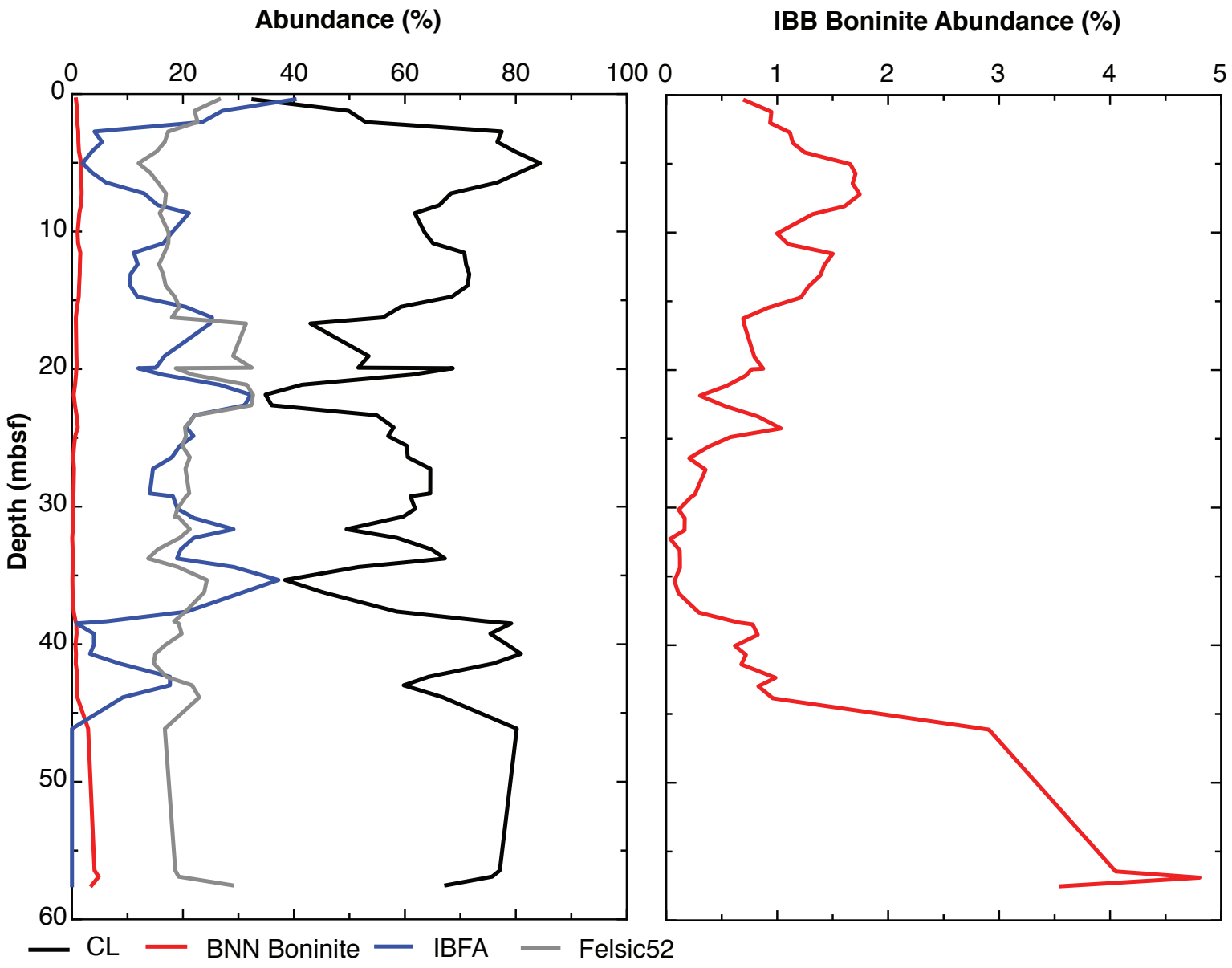
Abundance (%)
0
20
40
60
80
100
IBB Boninite Abundance (%)
0
1
2
3
4
5
Depth (mbsf)
0
10
20
30
40
50
60
CL
BNN Boninite
IBFA
Felsic52